Impact of Contact Interface Conditions on the Axial Load Bearing Capacity of Grouted Connections

Prof. Peter Schaumann, Alexander Raba, Anne Bechtel

ForWind - Center for Wind Energy Research
Institute for Steel Construction
Leibniz University Hannover
stahlbau@stahl.uni-hannover.de

Abstract

Grouted joints used in lattice support structures such as tripods or jackets for offshore wind turbines demand for reliable and economic design regulations. Current standards are not valid for executed geometries and used grout material due to the experimental background for which the design approaches were developed. Moreover, fatigue capacities of grouted joints are estimated without an acknowledged design model. To improve the design regulations for predominantly axial loaded grouted connections, a research project is conducted at the Institutes for Steel Construction and Building Materials Science, Leibniz University Hannover. Within this project small and large scale grouted joint specimens are tested under fatigue loading conditions. Additionally, influencing factors of varying contact specification at the interface between steel and grout are investigated. This paper introduces the test setups and describes results of surface roughness measurements of the specimens. The measurements are within the expected ranges of surface roughness for steel. In addition, results from small scale tests conducted submerged in water are presented. It becomes apparent, that water at the interface between steel and grout significantly reduces the fatigue performance of grouted joints. As one reason, hydro lubrication reducing the friction coefficient between steel and grout and leading to higher stress concentrations can be stated. Furthermore, a dependency on the test load frequency was observed, so that higher frequencies have a negative impact on the fatigue performance.

Keywords: grouted joints, fatigue, contact interface, friction, surface roughness, surface irregularities, hydro lubrication.

1 Introduction

Germany aims for covering 30 GW of its energy demand by means of Offshore Wind Turbines in 2030. Therefore, over 100 offshore wind farms will be built within the German Exclusive Economic Zone during the next decade. Most of the farms will be located in water depths of more than 30 meters. As a consequence, the turbines' support structures have to transfer enormous dynamic loads from wind and waves into the seabed. For monopile support structures these water depths will lead to an increase of the pile diameter and finally the steel demand. Due to a higher structural stiffness at less steel demand lattice substructures like jackets or tripods are preferred for deeper water, see Figure 1.1.

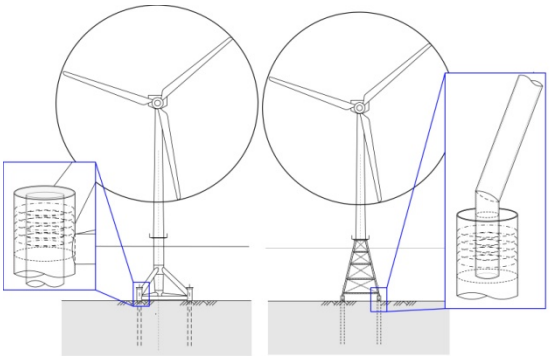

Figure 1.1: Grouted connection in tripod (left) and jacket (right) substructure of Offshore Wind Turbines.

Within the research project 'GROWup – Grouted Joints for Offshore Wind Energy Converters under reversed axial loadings and up scaled thicknesses' (funding sign: 0325290) sponsored by the German Federal Ministry for the Environment, Nature Conservation and Nuclear Safety (BMU) small and large scale tests on grouted joints under axial fatigue loading conditions are conducted.

Large-scale bending tests of Grouted Joints conducted in the previous research project 'GROW' (funding sign: 0327585) showed influences of interface conditions between steel and grout on the load bearing behaviour of the connection. These observations where confirmed by investigations of DNV [7].

Within 'GROWup' the transferability of the prior observations to axially loaded Grouted Joints will be examined. Therefore, the investigations include, but are not limited to reveal the impact of the interface conditions between steel and grout on the connection's reliability. The present paper provides first results from this project.

2 Grouted Joints

A common connection between substructure and foundation pile is the grouted joint (cf. Figure 1.1). This connection consists of an outer tube (sleeve) and a smaller inner tube (pile). The gap between pile and sleeve is filled with a high performance grout leading to a force fitted connection between the two tubes. For connections using plain surfaces of the steel tubes, loads are transferred from pile to grout and grout to sleeve by contact friction. Due to uncertain surface properties of the steel tubes, a decrease of surface roughness under cyclic loading and failing joints with plain steel surfaces in monopiles, it is strongly recommended to equip the steel tubes with shear keys usually made of weld beads [1]. Between a shear key on the outer pile and one on the inner sleeve surface a diagonal compression strut occurs under axial loads. The horizontal part of the compression strut braces against the circumferentially confining tube stresses. By this, a defined and reproducible load transfer is ensured which can also be described mechanically. When applying shear keys the acting axial load can be virtually split into several compression struts [2].

Grouted joints in monopiles are mainly loaded by bending moments while grouted joints in jackets and tripods are dominantly axially loaded. To realize a sufficient and easy installation in large water depths, the diameter to thickness ratio of the grout layer is rather large for lattice substructures. Even if the grouted joint is well known from the oil and gas industry only little data on the fatigue capacity of axially loaded grouted joints is available. Furthermore, previous investigations were carried out on grouted connections using geometries with small grout annulus and grout material strengths less than grouted joints and materials currently used in structures for offshore wind turbines.

Also little knowledge is available on the impact of the contact interface conditions on the axial load bearing capacity. First of all, the contact interface is influenced by the tubes' surface roughness and irregularities depending on the fabrication process. Second of all, grouted joints in lattice substructures are fully submerged in seawater. Cyclic loads and resulting movements of the grouted joint may lead to a pumping effect that spills water into the contact interface. This causes a modification of the friction conditions due to hydro lubrication. Additionally, cavitation and pure water pressure lead to an inner attrition of the grout.

3 State of Standardisation

Current design standards covering axial loaded grouted connections such as DNV-OS-J101 [3], ISO 19902 [4] and NORSOK N-004 [5] are applicable for grouted connections with a grout diameter to grout thickness ratio of $D_g/t_g \geq 10$. The applicability of the guidelines is limited to grout materials with compressive strengths $f_{cu} \leq 80$ MPa. These limitations and design procedures result from experimental investigations of Billington et al. [6], Lamport et al. [2]. In addition ISO 19902 and N-004 recommend an elastic modulus ratio of steel to grout of $E_s/E_g = 18$ if no further data is available. This ratio is based on tests conducted with cement slurry.

Table 1: Comparison of geometric proportions valid for application of ISO 19902 [4] and utilized in reference structures and test specimens.
Non valid values are marked in bold.

Geometric range of validity acc. to ISO 19902 [4]			Reference		Specimens		
			Jacket	Tripod	Small scale	Large Scale 1	Large Scale 2
20 ≤	D_p / t_p	≤ 40	20	**50**	**6.6**	**16**	24
30 ≤	D_s / t_s	≤ 140	37	64	**16.9**	41	41
10 ≤	D_g / t_g	≤ 45	**4**	10	**4.7**	**4**	**9.5**
1 ≤	L_e / D_p	≤ 10	2.7	1.3	1.5	1.5	1.5
	K	≤ 0.02	**0.08**	**0.03**	**0.09**	**0.07**	**0.04**
0 ≤	h / s	≤ 0.1	0.02	0.05	0.06	0.06	0.06
	h / D_p	≤ 0.012	0.01	0.01	**0.02**	0.01	0.01
				Scale	1:20	1:2	1:4

Current prevailingly axial loaded grouted connections have a grout diameter to grout thickness ratio of $D_g/t_g \leq 10$. Used grouts have compressive strengths higher than $f_{cu} = 80$ MPa and an elastic modulus ratio of about $E_s/E_g = 4$. Shown design parameters underline the differences between current and old grouted joint specification (cf. Table 1).

Moreover, only DNV-OS-J101 [3] in its current version enables the designer to include surface irregularities for calculation of interface shear strength due to friction. But none of the design equations consider the influence of water at the interface between steel and grout. Therefore, the applicability of mentioned design regulations for current structures is questionable and their reliability is uncertain.

4 Small Scale Tests

4.1 Introduction

By means of small scale tests (cf. Figure 4.1) the impact of high strength materials, surface roughness and irregularities on the fatigue performance as well as effects of hydro lubrication are investigated. Small scale specimens are grouted joints with a scale factor between 1:15 – 1:20 of a real connection. The test samples are equipped with shear keys. Due to the small geometries these shear keys are turned out of the tubes instead of weld beads.

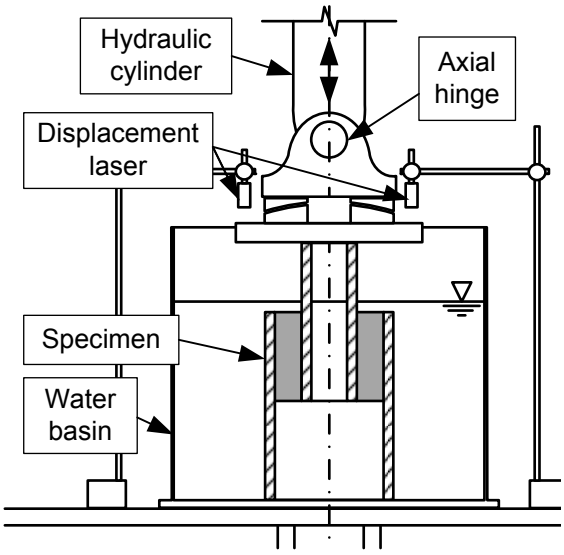

Figure 4.1: Small scale test setup with submerged specimen in water basin.

4.2 Test procedure

After machining the tube, surface roughness and irregularities of the specimens are tactilely measured (cf. Figure 4.2). Subsequently, the specimens are filled with grout and stored in a water basin. After 28 days of curing the characteristic axial load bearing capacity F_{ULS} is determined in a quasi-static compression test. In the following fatigue tests the upper compression limit is set to $0.5 \cdot F_{ULS}$. At this load level the specimens are cyclically loaded with a uniform compressive load level of R = 0.05 for 2 million cycles (runners) or until failure. Besides dry, small scale tests are also investigated under wet conditions, fully submerged.

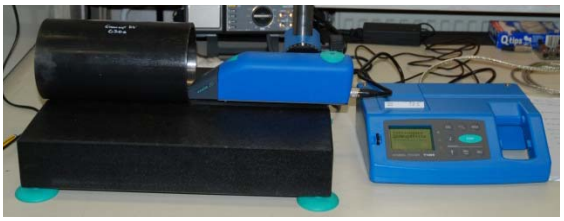

Figure 4.2: Tactile surface roughness measurement tool and sleeve tube of small scale specimen.

The test procedure will be conducted for two grout materials with different compressive strengths. Within this paper results for the grout material with lower compressive strength are presented. The material parameters are given by the producer as follows:

- compressive strength f_{cu} = 90 MPa
- tensile strength f_t = 6 MPa
- modulus of elasticity E_c = 40'000 MPa
- Poisson's ratio ν = 0.18

4.3 Results

4.3.1 Roughness and Irregularities

Results of the tactile roughness measurements are given in Figure 4.3. The turning process to fabricate the shear keys leads to smooth surfaces with an arithmetic mean roughness of $R_a \approx 2.3$ µm for the pile and $R_a \approx 5.0$ µm for the sleeve. The slightly higher and more varying roughness of the sleeve can be explained by the turning process itself. While the shear keys of the pile are turned out off the outer surface, the shear keys of the sleeve are turned out off the inner surface. The outward oriented position of the cutting tool is less favourable and leads to less precise results. Nevertheless all measured values are within the expectable range given in DIN 4766-2 [7] as 0.8 µm ≤ R_a ≤12.5 µm for turning machining.

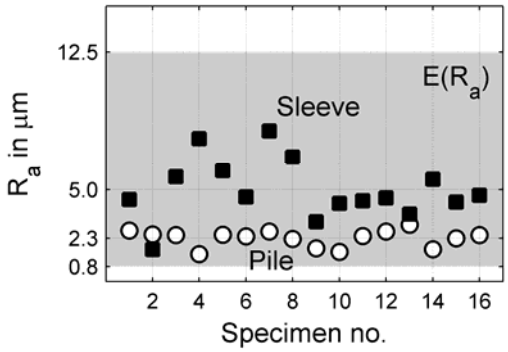

Figure 4.3: Arithmetic mean roughness R_a of small scale specimens and expectancy area for R_a of turning machining according to DIN 4766-2 [7].

4.3.2 Roughness versus F_{ULS}

Figure 4.4 shows a comparison of axial load bearing capacity of the grouted joints F_{ULS} with measured surface roughness R_a.

Pile surface roughness from specimens 4, 10 and 15 increases slightly similar to the axial load bearing capacity. A relation between surface roughness and axial load bearing capacity can be assumed. For specimen 2 and the sleeves' surface roughness of all specimens this relation cannot be confirmed.

Due to its smaller area compared to the sleeve, the interface between pile and grout is decisive for the axial and so the contact capacity. Due to the small variation of the pile's contact surface roughness (cf. Figure 4.3) the impact of the surface roughness on the axial ultimate capacity cannot be quantified.

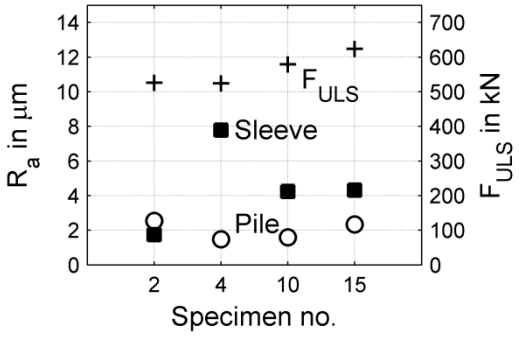

Figure 4.4: Comparison between surface roughness R_a and axial load bearing capacity FULS.

4.3.3 Dry versus wet

Figure 4.5 shows the absolute axial displacement at top of the specimen plotted over the number of cycles N. All specimens consist of the same grout material (cf. Section 4.2) and were loaded with 0.5 · F_{ULS}, R = 0.05 and 5 Hz. The two tests under dry conditions (cf. Figure 4.5: specimen no. 8 & 16) show no significant fatigue behaviour. After an initial settling within the first 5 to 10 thousand load cycles, more or less constant displacements can be measured. This behaviour is preserved till the test's end after 2 million load cycles. This leads to the assumption of appropriate fatigue strength for small scale specimens under dry conditions, if the fatigue load does not exceed 50 % of the ultimate axial load capacity of the small scaled grouted joints. Schaumann et al. [9] determined the same results for a higher test frequency of 10 Hz.

Contrary to this, the specimens tested under wet conditions (cf. Figure 4.5: specimen no. 6 & 11) show much larger displacements and a significantly lower fatigue resistance. Specimen no. 6 starts at a similar displacement level like specimen 16. After ten thousand load cycles the first compression strut fails and the displacement evolution is increased significantly until the second compression strut fails at a displacement of ~ 2.2 mm. After that, the specimen has no further load bearing capacities for the applied load level.

To confirm the result of specimen 6 a second specimen (no. 11) was tested under the same conditions. Specimen 11 shows a comparable behaviour but with a higher load bearing capacity of the first compression strut, failing at a displacement of ~ 1.3 mm. The second strut fails also at an axial displacement of ~ 2.2 mm. A slight hardening of the specimen at about N = 23'000 load cycles can be seen. This can be explained by locking of grout chunks between intact grout core and steel tube.

Nevertheless, the load bearing lifetime of both specimens under wet conditions tested at 5 Hz is limited to about N = 30'000 load cycles and therefore, is not suitable for application under cyclic loading for this fatigue load level.

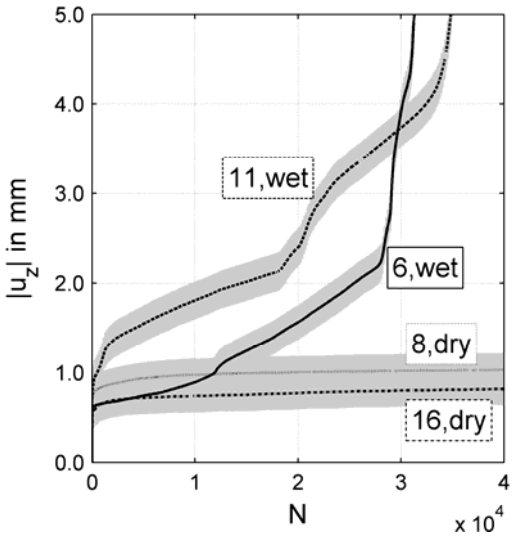

Figure 4.5: Axial displacement over number of cycles for specimens tested under dry and wet conditions.

4.3.4 Influence of Friction

The different behaviour of the grouted connection specimens when tested under wet conditions compared to dry conditions might be explained by hydro lubrication of the contact interface between steel and grout. Hence, numerical investigations are conducted focusing on the effect of the friction coefficient μ.

The numerical investigations are carried out using the finite element software ANSYS® and an axisymmetric specimen description (cf. Figure 4.6). A bilinear material law is applied to the steel parts with material parameters of an S355 structural steel. The 2-parametric Drucker-Prager failure surface is applied to the grout using material parameters according to Chen [10]. For contact the Coulomb friction law is used.

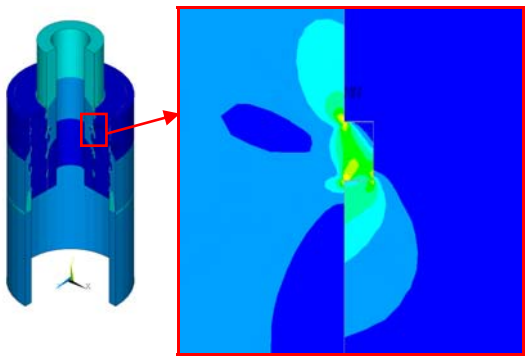

Figure 4.6: Numerical model showing σ_{int} distribution and shear key (right).

Figure 4.7 shows numerical results for μ varied between 0 and 1. A value of μ = 0 can be considered as theoretical example since friction is physically unavoidable. The asterisk marked line presents the absolute axial displacement at specimen top $|u_z|$ while the diamond marked line presents the maximum Tresca equivalent stress within the grout related to the grout's compressive strength σ_{int} / f_{cu}.

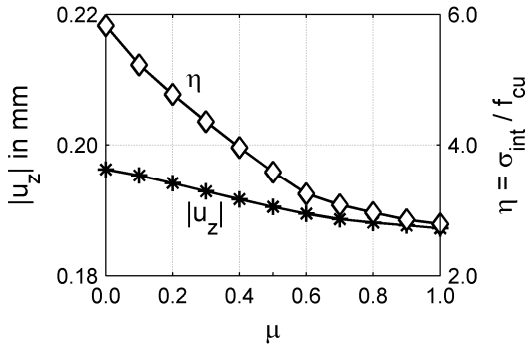

Figure 4.7: Axial displacement at specimen top and utilisation ratio of grout for varying friction coefficient.

The friction coefficient shows only little influence on the global displacement in a range of 10 μm. Considering, that the tests showed an axial displacement range of ~ 1 mm between the failure of two compression struts the influence of μ on the global displacement can be neglected. In contrast to that the Tresca equivalent stress shows a variation of the utilisation ratio of about 3 between μ = 0 and μ = 1. But it has to be kept in mind the distinct shear key of the small scale specimen (cf. Figure 4.6).

In DNV-OS-J101 [3] a friction coefficient μ = 0.4 for ultimate limit state calculations and μ = 0.7 for calculation of local tensile stresses is recommended. For consideration of long term friction between steel and grout μ should not exceed 0.4. A distinction between dry and wet interfaces is not made. Rabbat et al. [11] recommend μ = 0.57 for dry interfaces and μ = 0.65 for wet interfaces. Based on these recommendations the Tresca equivalent stress distribution σ_{int} in the grout for μ = 0, 0.4 and 0.7 is plotted in Figure 4.8.

It shows that the global stress distribution is not influenced by the friction coefficient, which explains the little influence of μ on the global displacement. The local stress distribution therefore is limited to small areas in front of the shear keys and shows great dependence on μ. Assuming, in contrast to the results of Rabbat et al. [11], that hydro lubrication reduces the friction coefficient this reduction increases local stress peaks and might lead to faster degradation of the grout around the shear keys.

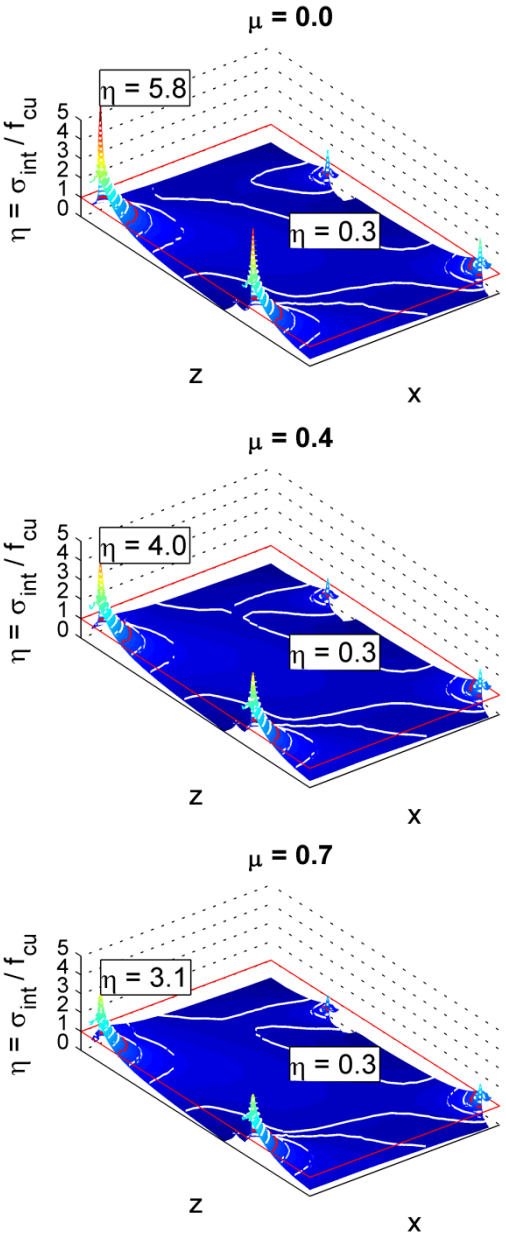

Figure 4.8: Distribution of utilisation ratios between a pair of shear keys for different friction coefficients.

5 Large Scale Tests

5.1 Introduction

The load and fatigue bearing behaviour of grouted connections with large grout annulus, currently installed to connect jacket and tripod structures with driven piles, is going to be investigated by conducting large-scale tests at the Institute for Steel Construction in cooperation with the Institute for Building Materials Science in the near future. The test set-up consists of outer tube (sleeve) and inner loaded tube (pile) equipped with shear keys on the facing surfaces (cf. Figure 5.1). The annulus between the steel tubes is filled with a high performance grout whereas two different materials with rather high and comparable low compression strength will be used. The main focus of the large-scale tests, the large grout annulus reflecting current geometries of tripods and jackets with a large annulus, is considered by two different annulus sizes. Besides grout annulus and material strength different shear key settings are investigated. The total size of the test bodies represents a scale of ~1:2 with a maximum grout thickness of 180 mm (360 mm origin). A scale of ~1:2 means a grouted joint with an overlapping length of L_g = 1240 mm, further geometrical dimensions are presented in Table 2.

Table 2: Geometries of large-scale specimens.

	Outer pile (Sleeve)	**Grout**	**Inner pile**
Outer Diameter D [mm]	~813	~773	~610/ ~406
Thickness t [mm]	~20	~80/ ~180	~25
Overlapping length L_g [mm]	~1240		

Due to the determined influence of interface conditions between grout and steel to the axial capacity before and after testing the roughness of the steel tubes were measured and studied. First effects of the surface conditions were analysed within the research work of previous project ‘GROW’ and the international research group by DNV [1].

5.2 Test procedure

Within preliminary investigations roughness measurements were conducted on inner sleeve and outer pile surface in the overlapping area. Surface irregularities and friction shall depict a design driving factor regarding the axial load capacity according to latest discussions and design revisions by DNV [3], [7]. Therefore, experimental and numerical investigations of the large scale tests are used to analyze the impact of surface conditions to the load bearing capacity.

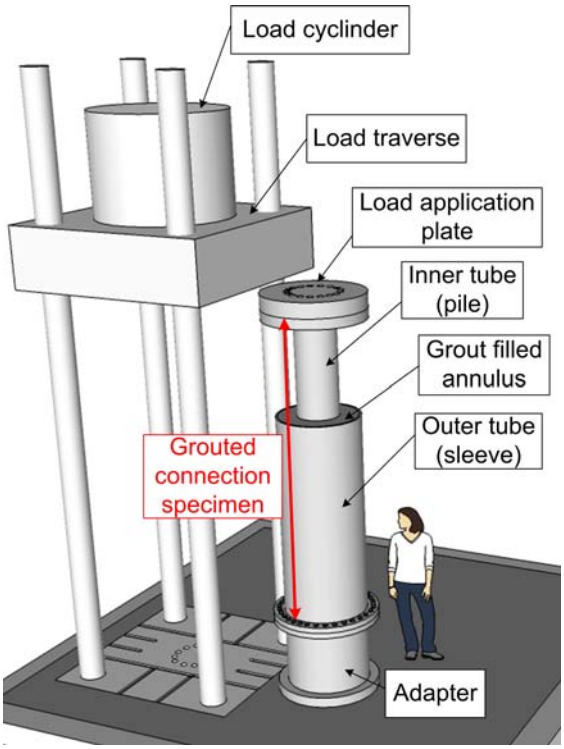

Figure 5.1: Large-scale test set-up and grouted connection specimen.

After preliminary investigations regarding the surface roughness the specimens are equipped with strain gauges, the pile is contrived into the sleeve and the annulus is filled with high performance grout. The fatigue behaviour of the grouted connection specimens will be analyzed by a progressively increased dynamic axial load. Within the first load levels full reversal loading (R = -1) with up to 3 MN effects the test bodies followed by a dynamic compression loading with R = -0.5 and a maximum compression load of -6 MN. Every load level consists of at least 100’000 load cycles. The maximum dynamic load reflects 60 % of

the ultimate limit state load F_{ULS} for the grouted connection specimen. In relation to real loading conditions the design load case (DLC) 6.1 acc. to IEC 61400-3 [12] was decisive for the reference structure whereas the applied test loads represent 35 % of the upper load $F_{dyn,u}$ and 45 % of the lower load $F_{dyn,l}$ regarding the reference load of an BSH-storm [13] combined with wave loads (BSH is the Federal Maritime and Hydrographic Agency responsible for approvals in the German Exclusive Economic Zone). Hence, the grouted connection is supposed to fail within the test procedure.

5.3 First Results

5.3.1 Numerical Investigations

First numerical investigations with the finite element software ANSYS® were conducted focusing on the load bearing behaviour of the test specimens under static and fatigue loading. The large-scale specimen was implemented similar to the small-scale specimen described in Section4.3.4. For the surface roughness a friction coefficient μ = 0.4 according to latest recommendations by DNV [3] were considered. Comparison of small and large grout annulus calculations showed that arising compression struts between opposite shear keys are not established significantly within the large grout annulus (t_g) as can be seen by comparing left and right numerical stress plot of Figure 5.2. The stress distribution is more uniform over all shear keys and the contact area, cf. Figure 5.2 right plot of numerical results.

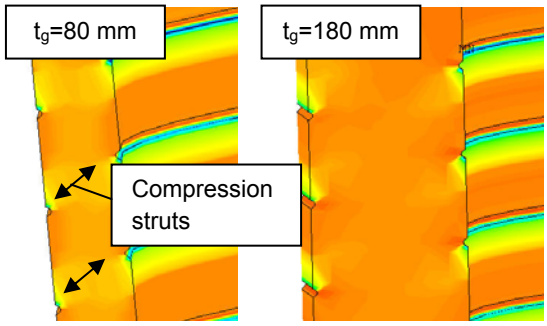

Figure 5.2: Numerical results showing principal stress distribution for grout annulus t_g = 80 mm (left) and t_g = 180 mm (right) representing test specimen geometries.

Therefore, further investigations regarding the influence of surface conditions to the load bearing and failure behaviour will be performed. The numerical model will be validated by the first large-scale test results. Considering the fatigue behaviour local crushing effects and grout damage in the area of the shear keys are expected as numerical investigations indicated [14].

5.3.2 Tactile Roughness Measurements

The steel tubes used for the large-scale tests originate from an experienced fabricator producing steel tubes for offshore wind turbines. The steel tubes were cold rolled merged to a steel tube with longitudinally submerged arc-welds. The surfaces were not treated and revealed a rather irregular state influenced by corrosion. Before the tactile roughness measurements the surfaces were cleaned to remove loose particles. The surfaces are not sand blasted since real structures resting dockside corrode. No surface treatment takes place before installation. Therefore the corroded surface of the specimens was kept to include realistic assumptions.

The performed tactile roughness measurements at the inner surface of the sleeve and the outer surface of the pile on varied locations showed for all measurements an aperiodic surface profile with a limit wavelength of 2.5 mm.

Figure 5.3 to Figure 5.5 present the main roughness parameters for pile and sleeve of the first large-scale grouted connection specimen. The sleeve roughness reaches for all three roughness parameters higher values than for the pile. Hence, the sleeve surface is rougher due to the inner location and the effect of the rolling. Contrary to the sleeve roughness, showing a rather small spread of measurements, the pile roughness values are clearly spread over a wider range. This may result from the outside location on the pile being more influenced by mechanical effects.

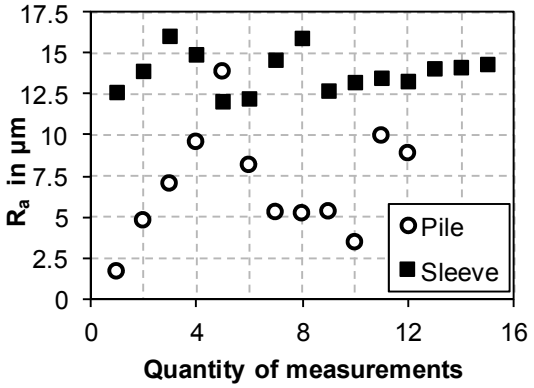

Figure 5.3: Arithmetical mean deviation R_a for pile and sleeve of the first large-scale grouted connection specimen.

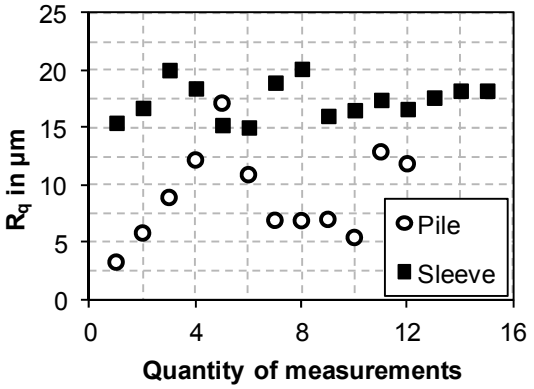

Figure 5.4: Quadratic mean deviation R_q for pile and sleeve of the first large-scale grouted connection specimen.

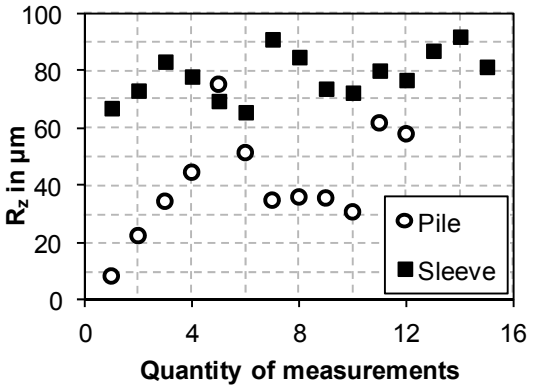

Figure 5.5: Average roughness depth R_z for pile and sleeve of the first large-scale grouted connection specimen.

The arithmetical mean deviation R_a depicted in Figure 5.4 has for the sleeve an average of ~ 13 µm which is in the range of usual rolled steel (0.15 – 25 µm) according to DIN 4766-2 [7]. Whereas R_a for the pile surface has an average value of ~ 7 µm which is rather small compared to the sleeve value but still in the range of rolled steel tubes. The arithmetical mean deviation reflects only a highly averaged value. Hence, for a more specific analysis the average roughness depth and the quadratic mean deviation are presented in Figure 5.4 and Figure 5.5. The average roughness for the sleeve is ~ 73 µm and for the pile with a larger spread ~ 40 µm. Both values represent the upper range for rolled steel tubes (1 – 100 µm) according to 4766-2 [7]. The quadratic mean deviation, comparable to the statistical standard deviation, is in this case highly influenced by significant tops and valleys of the roughness profile.

6 Conclusions

Conducted investigations on the surface roughness regarding small-scale specimens show that little deviations have no direct influence on the load bearing capacity of grouted joints when shear keys are applied. The smooth surface produced by the turning process allows little interlocking between grout and steel. The large-scale specimens show slightly higher surface roughness and its influence on the load bearing capacity might be more obvious. Test results from future tests will give insights.

The small scale tests reveal a high impact on the number of endurable cycles under fatigue loading (dry: N = 2 m.; wet: N = 30 k.) when tested submerged in water. One possible aspect might be hydro lubrication in the contact interface, leading to increasing local stresses and therefore a faster degradation of the grout. Moreover, the degradation might be accelerated by local overpressure of water within the contact interface and resulting cavitation. These effects might be significantly influenced by the applied test frequency.

In further small-scale investigations the surface roughness of specimens with and without shear keys will be measured. This will enable a broader base for the described results. Moreover the frequency dependency of submerged cyclic loading tests will be investigated and brought to frequency ranges occurring in real substructures.

With regard to the large-scale tests the tactile roughness measurements will be compared to the test results of the dynamic large-scale tests and published test data. In addition to the tactile measurements optical measurements and three dimensional analyses are going to be conducted by a digital microscope. Both roughness measurements are going to be analyzed further in numerical investigations to reveal the influence on the load bearing capacity regarding the ultimate and fatigue limit state.

Acknowledgement

The presented results and approaches are achieved within the research project 'GROWup - Grouted Joints for Offshore Wind Energy Converters under reversed axial loadings and up scaled thicknesses' (funding sign: 0325290) funded by the German Federal Ministry for the Environment, Nature Conservation and Nuclear Safety (BMU). The authors thank the BMU for financing and all accompanying industry project partners (Fraunhofer IWES, GL, REpower, RWE Innogy, Strabag) for their support.

References

[1] Schaumann, P. et al. (2010): Sinking grouted joints in offshore wind turbines – Bearing behaviour, repair, and optimisation, Stahlbau 79, Heft 9, Ernst & Sohn Verlag, Berlin, 2010. (in German)

[2] Lamport, W. B., Jirsa, J. O., Yura, J. A.: Grouted Pile-to-Sleeve Connection Tests, Report on a Research Project, PMFSEL Report No. 86-7, Department of Civil Engineering, University of Austin in Texas, United States of America, June 1986.

[3] Det Norske Veritas: Offshore Standard DNV-OS-J101 - Design of Offshore Wind Turbine Structures, Høvik, Norway, September 2011.

[4] DIN EN ISO 19902: Erdöl- und Erdgasindustrie – Gegründete Stahlplattformen, DIN Deutsches Institut für Normung e.V., July 2008. (in German).

[5] NORSOK N-004: Design of steel structures – Annex K: Special design provisions for jackets. Revision of section K.5.3 Grouted connection, Standards Norway, Lysaker, Norway, April 2012.

[6] Billington, C.J., Lewis, H. G.: The Strength of Large Diameter Grouted Connections, Proceedings of the 10th Annual Offshore Technology Conference, Houston, USA, 1978.

[7] Det Norske Veritas: Technical Report – Joint Industry Project – Summary Report from the JIP on the Capacity of Grouted Connections in Offshore Wind Turbine Structures, Report No. 2010-1053 rev. 05, Høvik, Norway, May 2011.

[8] DIN 4766-2: Herstellverfahren der Rauheit von Oberflächen – erreichbare Mittenrauhwerte Ra nach DIN 4768 Teil 1, DIN Deutsches Institut für Normung e.V., March 1981. (in German).

[9] Schaumann, P.; Bechtel, A.; Lochte-Holtgreven, S.: Fatigue Performance of Grouted Joints for Offshore Wind Energy Converters in Deeper Waters, Proceedings of the Twentieth International Offshore and Polar Engineering Conference, Beijing China, pp. 672-679, 2010.

[10] Chen, W.F.: Plasticity in reinforced concrete, McGraw-Hill, New York, 1982.

[11] Rabbat, B.G.; Russell, H.G.: Friction Coefficient of Steel on Concrete or Grout, Journal of Structural Engineering, Issue 3, pp. 505-515, ASCE, 1985.

[12] IEC 61400-3: Wind turbines – Part 3: Design requirements for offshore wind turbines, International Electronical Commission, April 2009.

[13] Bundesamt für Seeschifffahrt und Hydrographie (BSH): Anwendungshinweise für den Standard „Konstruktive Ausführung von Offshore-Windenergieanlagen" des BSH (aktualisierte Fassung), (http://www.bsh.de/de/Produkte/Buecher/Standard/Anlage1.pdf). Hamburg, Germany, 2012.

[14] Schaumann, P.; Bechtel, A.; Lochte-Holtgreven, S.: Grouted Connections with Large Annulus in Offshore Wind Turbines and Substations, Proceedings of the 11th German Wind Energy Conference DEWEK 2012, Bremen, Germany, 2012.